ACS OMEGA

http://pubs.acs.org/journal/acsodf

Article

Inhibition of Inflammatory Response and Promotion of Osteogenic Activity of Zinc-Doped Micro-Arc Titanium Oxide Coatings

Haishui Sun,○ Yiming Yang,○ Lei Yu, Ke Liu, Yifan Fei, Chaoyang Guo, Yuqi Zhou, Jingzhou Hu,* Lei Shi,* and Honghai Ji*

Cite This: *ACS Omega* 2022, 7, 14920−14932

Read Online

ACCESS | Metrics & More | Article Recommendations

ABSTRACT: An early and sustained immune response can lead to chronic inflammation after the implant is placed in the body. The implantable materials with immunomodulatory effects can reduce the body's immune response and promote the formation of ideal osseointegration between the implants and bone tissue. In this study, zinc-coated titanium micro-arc oxide coating was prepared on titanium surface by micro-arc oxidation. The physical properties, anti-inflammation, and osteogenesis of the material were evaluated. We have physically characterized the surface structure of the coatings by scanning electron microscopy (SEM), energy-dispersive X-ray spectroscopy (EDS), and atomic force microscopy (AFM) and detected the release of Zn^{2+} from the coating surface by inductively coupled optical plasma emission spectrometry (ICP-OES). The BMSCs were inoculated on the surface of the coating, and the biocompatibility of the coating was evaluated by CCK-8 analysis and living and dead cell staining. The osteogenic effect of the layer on BMSCs was evaluated by alkaline phosphatase (ALP) assays, osteocalcin (OCN) immunofluorescence, and quantitative polymerase chain reaction (q-PCR). The survival status of RAW264.7 on the coating surface and the mRNA expression of the associated proinflammatory markers, tumor necrosis factor-α (TNF-α), cluster of differentiation 86 (CD86), and inducible nitric oxide (INOS) were detected by CCK-8 analysis and q-PCR. In parallel, the cell counting kit-8 (CCK-8) analysis and q-PCR screened and evaluated the effective concentration of Zn^{2+} anti-inflammatory in vitro. The results show that the coating has good physical characterization, and Zn is uniformly bound to the surface of titanium and shows stable release and good biocompatibility to BMSCs, downregulating the expression of inflammation-related genes promoting the bone formation of BMSCs. We have successfully prepared zinc-coated micro-arc titanium oxide coating on the titanium surface, which has good osteogenesis and great anti-inflammatory potential and provides a new way for osseointegration in the implant.

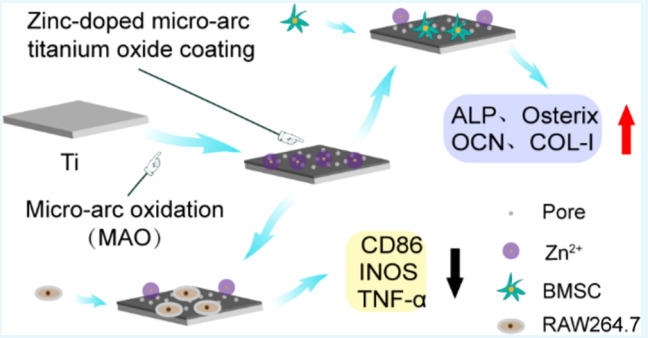

1. INTRODUCTION

Titanium has excellent biocompatibility and is the standard carrier for dental implant materials and is currently considered the metal of choice for dental implants.[1,2] However, titanium lacks biological activity and, when implanted in the body, is more mechanically bonded to bone tissue and does not form osseointegration.[3] When planted as foreign bodies, titanium implants inevitably cause an immune response in the host.[4] When the implant is placed, the host immune response is activated, and the continued activation of the immune system leads to chronic inflammation and the destruction of healthy tissue around the implant.[5,6] It is increasingly essential to modulate the host immune response, reduce the release of local inflammatory factors, and decrease the expression of inflammatory genes during the initial implant placement phase.

As the primary effector cell in the biological response of the implanted material, macrophages determine the success or failure of the injected material to some extent.[7] It has been found that soft tissue biopsies around orthopedic and oral implants show a severe inflammatory response around titanium particle aggregates.[8] In addition, the scattered Ti particles around the dental implants could promote the expression of proinflammatory cytokines.[8] It was found that the immune microenvironment can be regulated by modulating the surface microstructure, wettability, particle size, porosity, and released ions of biomaterials.[9−11] As titanium implants, it has also been

Received: January 28, 2022
Accepted: March 22, 2022
Published: April 19, 2022

found that changing the titanium surface morphology and wettability can modulate the activation of macrophages.[5]

Zinc (Zn), a trace element essential to the function and structure of the body, performs a variety of positions in growth, immunity, tissue maintenance, and wound healing.[12] Zinc has good bone-enhancing properties and excellent antibacterial activity,[13,14] effectively preventing postoperative infections.[12] At the same time, zinc ions also have anti-inflammatory activity, reducing the inflammatory response by reducing the production of proinflammatory cytokines and enhancing the secretion of anti-inflammatory cytokines.[15−17] It has been found that the addition of a layer of zinc ions to sulfonated polyether ether ketone (SPEEK) biomaterials modulates the shift in the polarization of nonactivated macrophages toward an anti-inflammatory phenotype and induces the secretion of anti-inflammatory and osteogenic cytokines.[18]

Micro-arc oxidation (MAO) technology can produce porous TiO_2 coatings on Ti surfaces with good biocompatibility and biomechanical properties that modulate the osteogenic ability of the surface.[19,20] However, TiO_2 nanotubes with different properties (crystallinity) exhibit different osteogenic effects on rat BMSCs.[21] MAO can also form a micro-arc titanium oxide coating with multiple hollow channels on the titanium alloy surface, providing a suitable carrier for loading ions, drugs, and peptides.[22,23] Previous studies on Zn-coated micro-arc titanium oxide coatings have focused more on antibacterial aspects than modulating the inflammatory response.[3,24] For this reason, we combined Zn on the titanium surface to investigate its anti-inflammatory and pro-osteointegration effects.

In this study, we used micro-arc oxidation technology to form Zn-coated micro-arc titanium oxide coating on the titanium surface, where Zn is mainly present on the porous TiO_2 coating surface in the form of ZnO, which will be released into the environment as Zn^{2+} when cocultured with cells.[25,26] By the micro-arc oxidation technology, we loaded the element Zn on the titanium surface, and through the release of Zn^{2+}, we formed a local anti-inflammatory microenvironment on the implant surface, reducing the host's immune rejection at the early stage of implant placement, weakening the associated inflammatory response, and promoting bone regeneration. The prepared Zn-coated micro-arc titanium oxide coating's physical characterization, biocompatibility, osteogenesis, and anti-inflammatory effects were evaluated. In addition, the optimum concentration of Zn^{2+} was screened for its anti-inflammatory impact on RAW264.7 cells in vitro. It further suggests that Zn^{2+} plays an anti-inflammatory role on the surface of the micro-arc oxide coating.

2. MATERIALS AND METHODS

2.1. Preparation of Materials. The square titanium plate (10 mm × 10 mm × 1 mm) selected in this study was from commercially pure titanium plates. First, 400−2000 # sandpaper was used to polish the surface of titanium wafers. The characters were washed with acetone, ethanol, and distilled water for 15 min and then dried. To prepare the micro-arc oxidation coating, the electrolyte is a mixture of 0.2 mol/L calcium acetate monohydrate ($C_4H_6CAO_4H_2O$, Macklin, Shanghai, China) and 0.04 mol/L sodium pentahydrate β-glycerophosphate ($C_3H_7NA_2O_6P{\cdot}5(H_2O)$, Macklin, Shanghai, China). The Zn group (5, 10 mmol/L) was supplemented with zinc acetate (Zn $(CH_3COO)_2$ $2H_2O$, Macklin, Shanghai, China). Zn^{2+} groups were named Zn1 (5 mmol/L) and Zn2 (10 mmol/L). The voltage is set to 360 V, the frequency is 200 Hz, 30% duty cycle, and 2 min.

2.2. Material Surface Characteristics. To analyze the physical characterization of the coating, the surface morphology of the micro-arc oxide coating was observed by a scanning electron microscope (SEM) (Hitachi, 3400N, Japan), the surface element distribution of the layer was analyzed by energy-dispersive X-ray spectroscopy (EDS) (Bruker, Germany), the wettability of the coating was measured by a contact angle meter (JY-82B Kruss DSA, Kruss, Hamberg, Germany), the surface roughness of the material coating was analyzed by an atomic force microscope (AFM) (Bruker Dimension Icon, Rheinstetten, Germany), and ImageJ (National Institutes of Health, Bethesda, MD) analysis indicated the pore size and pore distribution.

2.3. Release of Zn Ions. The titanium slices of MAO, Zn1, and Zn2 groups were immersed in the same volume (5 mL) of phosphate-buffered saline (PBS) and placed in a 37 °C environment. The entire solution was extracted on 1, 3, and 7 days. After each extraction, an equal amount of PBS solution was added again to continue the immersion. Ion release was measured by inductively coupled optical plasma emission spectrometry (ICP-OES) (Agilent 720ES).

2.4. Cell Culture. The Sprague Dawley (SD) rats used in the experiments were obtained from the Animal Centre of the Ninth People's Hospital of Shanghai Jiao Tong University, and animal ethical approval was obtained for all animal experiments performed. Necks of 3−5 week SD rats were broken and executed, alcohol-soaked for 5 min, tibia and femur were isolated, and primary BMSCs were obtained by the whole bone marrow apposition method. Primary BMSCs were cultured in 10% fetal bovine serum (FBS) (GIBCO, Australia) and 1% penicillin/streptomycin (P/S, GIBCO, Carlsbad, CA) in Dulbecco's modified Eagle's medium (DMEM) (HyClone, Logan, UT), and the fluid was changed after three days. The cells proliferated to 70−90% passages, and pure P_2−P_4 BMSCs were selected for subsequent experiments.

We purchased the RAW264.7 cell line from the Chinese Academy of Sciences (Shanghai, China) for testing. Cells were cultured in high-glucose DMEM containing 10% FBS and 1% P/S. The cell culture medium is replaced every three days and every two days. Both BMSCs and RAW264.7 were cultured at 37 °C and 5% CO_2.

2.5. Cell Counting Kit-8 (CCK-8) Assay and Live/Dead Fluorescence Staining. The biocompatibility of Zn-coated micro-arc titanium oxide was examined using CCK-8 analysis. BMSCs in good condition were inoculated at a density of 5 × 10^4/well in 24-well plates (Corning Costar Co., New York, NY) placed with Ti, MAO, Zn1, and Zn2. The absorbance was measured on 1, 3, and 7 days after culture. The medium was discarded and washed again with PBS. The medium containing 10% CCK-8 solution (DOJINDO, Kumamoto, Japan) was added to each well. After incubation at 37 °C, protected from light, and waiting for 2 h, the supernatant was pipetted onto a 96-well plate (Corning Costar Co., New York, NY), and the absorbance was measured at 450 nm using an enzyme analyzer.

To further examine the biocompatibility of Zn-coated micro-arc titanium oxide on cells, we took a live−dead cell staining method to observe the growth state of BMSCs on Zn-coated micro-arc titanium oxide. BMSCs were inoculated at a density of 5 × 10^4/well in 24-well plates placed with Ti, MAO, Zn1, and Zn2. The cells were cultured for 1 day and then stained. The supernatant was discarded, washed once with PBS, added

https://doi.org/10.1021/acsomega.2c00579
ACS Omega 2022, 7, 14920−14932

Table 1. Primers Used for the Evaluation of Osteogenesis-Related Gene Expression in BMSCs

gene	forward primer sequence (5′−3′)	reverse primer sequence (5′−3′)
ALP	ATGCTCAGGACAGGATCAAA	CGGGACATAAGCGAGTTTCT
osterix	CGGCAAGGTGTACGGCAAGG	GAGCAGAGCAGACAGGTGAACTTC
COL-I	AGCTCGATACACAATGGCCT	CCTATGACTTCTGCGTCTGG
OCN	CAGACAAGTCCCACACAGCA	CCAGCAGAGTGAGCAGAGAG
β-actin	CCTCTATGACAACACAGT	AGCCACCAATCCACACAG

Table 2. Primers for Evaluating the Expression of Inflammation-Related Genes in RAW264.7

gene	forward primer sequence (5′−3′)	reverse primer sequence (5′−3′)
INOS	ACTCAGCCAAGCCCTCACCTAC	TCCAATCTCTGCCTATCCGTCTCG
TNF-α	GCCTCTTCTCATTCCTGCTTGTGG	GTGGTTTGTGAGTGTGAGGGTCTG
CD86	TGTTTCCGTGGAGACGCAAG	TTGAGCCTTTGTAAATGGGCA
IL-1β	GCAACTGTTCCTGAACTCAACT	ATCTTTTGGGGTCCGTCAACT
GADPH	ACCCAGAAGACTGTGGATGG	CACATTGGGGGTAGGAACAC

to the prepared live−dead cell staining solution (Beyotime, Cat: C2015M, Shanghai, China), incubated for 30 min protected from light, and washed again with PBS. The staining of BMSCs by living and dead cells was observed by a light microscope (Olympus, Tokyo, Japan). At the same time, the living cells of BMSCs were counted by ImageJ software.

2.6. Cell Adhesion Analysis. To observe the adhesion effect of BMSCs on the material surface, we inoculated BMSCs on titanium sheets at a density of 5×10^4/well, and after 12 h of inoculation and fixed dehydration dry fabrication, Phenom (Phenom Pro, Phenom-World BV, Eindhoven, the Netherlands) was observed and photographed.

To further observe the adhesion of BMSCs on the material surface, the cytoskeleton was determined by staining β-actin with tetramethylrhodamine (TRITC)−phalloidin. BMSCs were inoculated at a density of 5×10^4/well and cultured in 24-well plates containing Ti, Mao, Zn1, and Zn2. After 7 days of incubation, the medium was aspirated, discarded, and washed three times using PBS. BMSCs were fixed using 4% paraformaldehyde for 30 min, permeabilized with 0.5% Triton X-100 for 20 min, and washed three times using PBS. Then, the cells were sealed with bovine serum albumin (BSA) for 1 h. Finally, TRITC (1:200; Yeasen, Shanghai, China) was incubated for 30 min protected from light, washed three times using PBS, and then, the cell nuclei were re-stained with DAPI (1:500; Solarbio, Beijing, China) for 5 min after fluorescence microscopy (TE2000-U, Nikon, Tokyo, Japan) images were taken.

2.7. ALP Activity Analysis and OCN Immunofluorescence Staining. Alkaline phosphatase (ALP) staining and ALP activity analysis were used to verify the osteogenic effect of zinc-coated micro-arc titanium oxide on BMSCs. BMSCs were inoculated at a density of 5×10^4/well and cultured in 24-well plates containing Ti, Mao, Zn1, and Zn2. After 7 days of culture, we operated according to the ALP staining kit (Beyotime, Shanghai, China) and ALP activity detection kit (Beyotime, Shanghai, China).

Immunofluorescence was used to detect the expression of OCN. BMSCs were seeded at a density of 5×10^4/well and cultured in a 24-well plate containing Ti, MAO, Zn1, and Zn2. After 7 days of incubation, the medium was aspirated, discarded, and washed three times using PBS. BMSCs were fixed using 4% paraformaldehyde for 30 min, permeabilized with 0.5% Triton X-100 for 20 min, and washed three times using PBS. Then, the cells were sealed with BSA for 1 h. The cells were then incubated with an anti-osteocalcin (OCN) (1:100, Affinity, Cincinnati, OH) overnight at 4 °C. After incubation overnight, the primary antibody was washed three times for 5 min each using PBS and then incubated with Alexa Fluor 555 donkey antirabbit antibody (1:200, Beyotime, Shanghai, China) for 1 h. The cells were washed three times with PBS and finally incubated with DAPI for 5 min. A fluorescence microscope (TE2000-U, Nikon, Tokyo, Japan) was used for measurements. The fluorescence intensity was acquired from images and quantitatively analyzed by ImageJ software.

2.8. Related Osteogenic Gene Expression. The expression of osteogenic genes was detected by reverse transcriptase-polymerase chain reaction (q-PCR). BMSCs were inoculated in 24-well plates containing Ti, MAO, Zn1, and Zn2 and cultured at 5×10^4 cells per well. The expression of relevant genes was detected on day 7 and day 14. First, total RNA was isolated using Trizol reagent (Invitrogen), followed by reverse transcription using PrimeScript RT reagent (Takara Bio Inc., Shiga, Japan). The expression of ALP, Osterix, collagen I (COL-I), and OCN associated with osteogenic differentiation was analyzed using real-time PCR (SYBR Premix EX Taq, Takara, Tokyo, Japan). Butler β-actin was used to normalize the results. Data are expressed as fold change of the control according to equation $2^{-\Delta\Delta Ct}$. The primer sequences of the genes mentioned in the experiments are shown in Table 1.

2.9. RAW264.7 Proliferative Activity and Growth Status. To study the status of RAW264.7 cells in zinc-coated micro-arc titanium oxide, we performed CCK-8 analysis. RAW264.7 in good condition was inoculated at 2×10^5/well in 24-well plates containing Ti, MAO, Zn1, and Zn2. The absorbance was measured after 24 h incubation. The medium was removed and washed using PBS. Briefly, 500 μL of medium containing 10% CCK-8 solution to each well was added. After incubation at 37 °C for 2 h under low light, the supernatant was aspirated into a 96-well plate, and the absorbance was measured at 450 nm with an enzyme analyzer.

To further observe the growth state of RAW264.7 on zinc-coated micro-arc titanium oxide, we performed live−dead cell staining of RAW264.7 cells. RAW264.7 was inoculated in 24-well plates containing different titanium sheets at the same density (2×10^5/well) and incubated for 24 h, and then, live−dead cell staining was performed. Pictures were taken under a

https://doi.org/10.1021/acsomega.2c00579
ACS Omega 2022, 7, 14920−14932

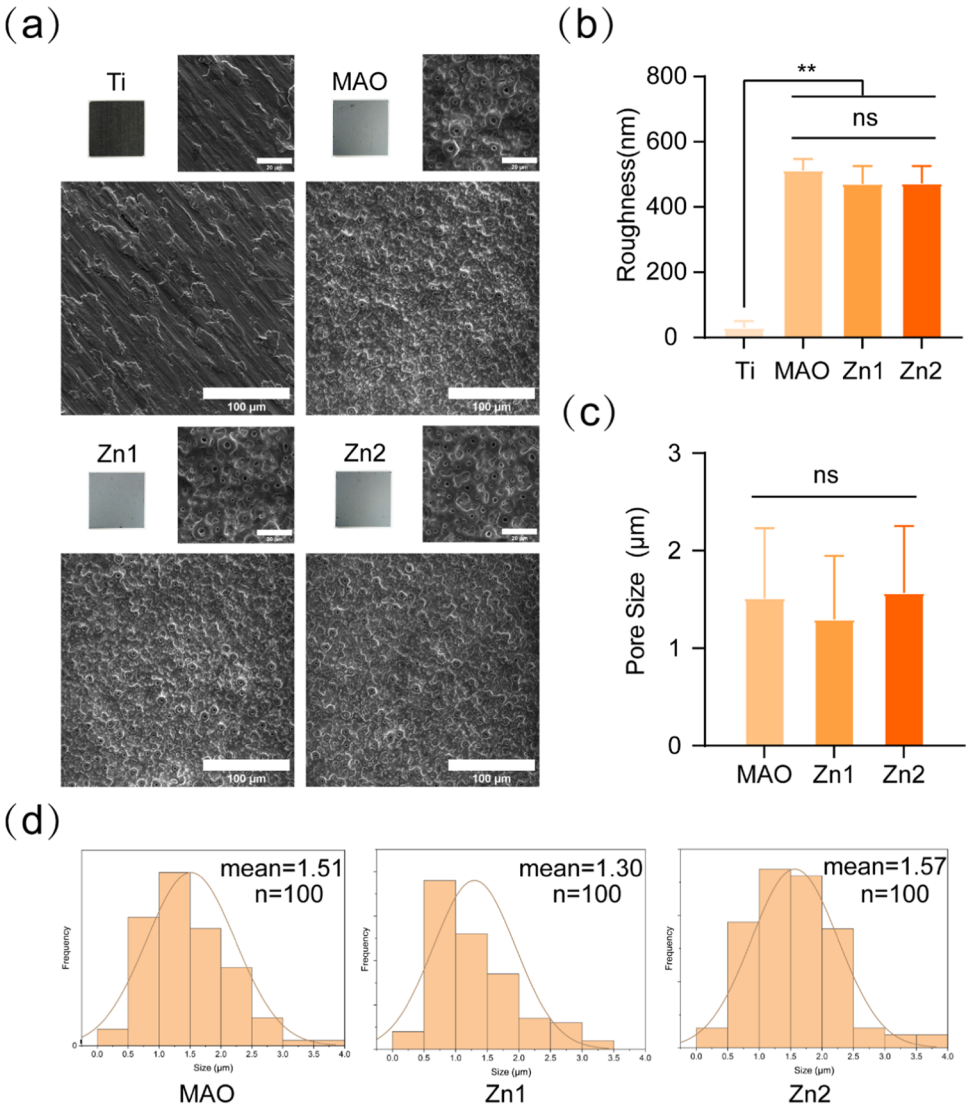

Figure 1. (a) Surface morphology of Ti, MAO, Zn1, and Zn2 was observed by the SEM. (b) Titanium and three different surface roughnesses. (c) Surface pore size of MAO, Zn1, and Zn2. (d) Frequency distribution of surface aperture in MAO, Zn1, and Zn2 (n = 100). $^{**}P < 0.01$, $^{*}P$ indicates significant difference between groups. NS indicates no significant difference between the compared groups. Scale bar: 20 and 100 μm.

fluorescence microscope, and statistical analysis of the percentage of live−dead cells was performed using ImageJ.

2.10. Related Inflammatory Gene Expression. RAW264.7 cells were seeded at a density of 2 × 10^5/well and cultured in a 24-well plate containing Ti, MAO, Zn1, and Zn2. The cells were continued to be refined for 24 h after. The expression of proinflammatory-related genes, inducible nitric oxide synthase (INOS), tumor necrosis factor-α (TNF-α), and the cluster of differentiation 86 (CD86), was evaluated by q-PCR. First, total RNA was isolated using Trizol reagent (Invitrogen), followed by reverse transcription using Prime-Script RT reagent (Takara Bio Inc., Shiga, Japan). The expression of genes was analyzed using real-time PCR (SYBR Premix EX Taq, Takara, Tokyo, Japan). GADPH was used to normalize the results. Data are expressed as fold change of the control according to equation $2^{-\Delta\Delta Ct}$. The primer sequences of the genes mentioned in the experiments are shown in Table 2.

2.11. Zn^{2+} Concentration Screening. To understand the effect of Zn^{2+} concentration on the anti-inflammatory effect, we screened Zn^{2+}. DMEM solutions containing Zn^{2+} at concentrations of 20, 40, 60, 80, 100, 120, 140, 160, and 180 μM were used to screen. DMEM without Zn^{2+} serves as the control. RAW264.7 cells were inoculated in 96-well plates (Corning Costar Co., New York, NY) at a density of 1 × 10^4/well, and then, the RAW264.7 cells were incubated for 1 and 3 days, and a 100 μL buffer containing 10 μL of CCK-8 reagent was added to each empty hole. After incubation at 37 °C for 2 h in the dark, the values were read at 450 nm by the enzyme-labeled analyzer.

2.12. Effect of Different Concentrations on the Expression of Inflammatory Genes. To investigate the effect of Zn^{2+} on the expression of relevant inflammatory genes, RAW264.7 was inoculated in six-well plates (Corning Costar Co., New York, NY) at a density of 5 × 10^5/well, and when the cells proliferated to about 80% of the well plates, they were intervened with DMEM containing Zn^{2+} concentrations of 40, 60, 80, and 100 μM for 3 days.

First, total RNA was isolated using Trizol reagent (Invitrogen), followed by reverse transcription using Prime-Script RT reagent (Takara Bio Inc., Shiga, Japan). The expression of proinflammatory-related genes, TNF-α, INOS, CD86, and IL-1β, was analyzed using real-time PCR (SYBR

https://doi.org/10.1021/acsomega.2c00579
ACS Omega 2022, 7, 14920−14932

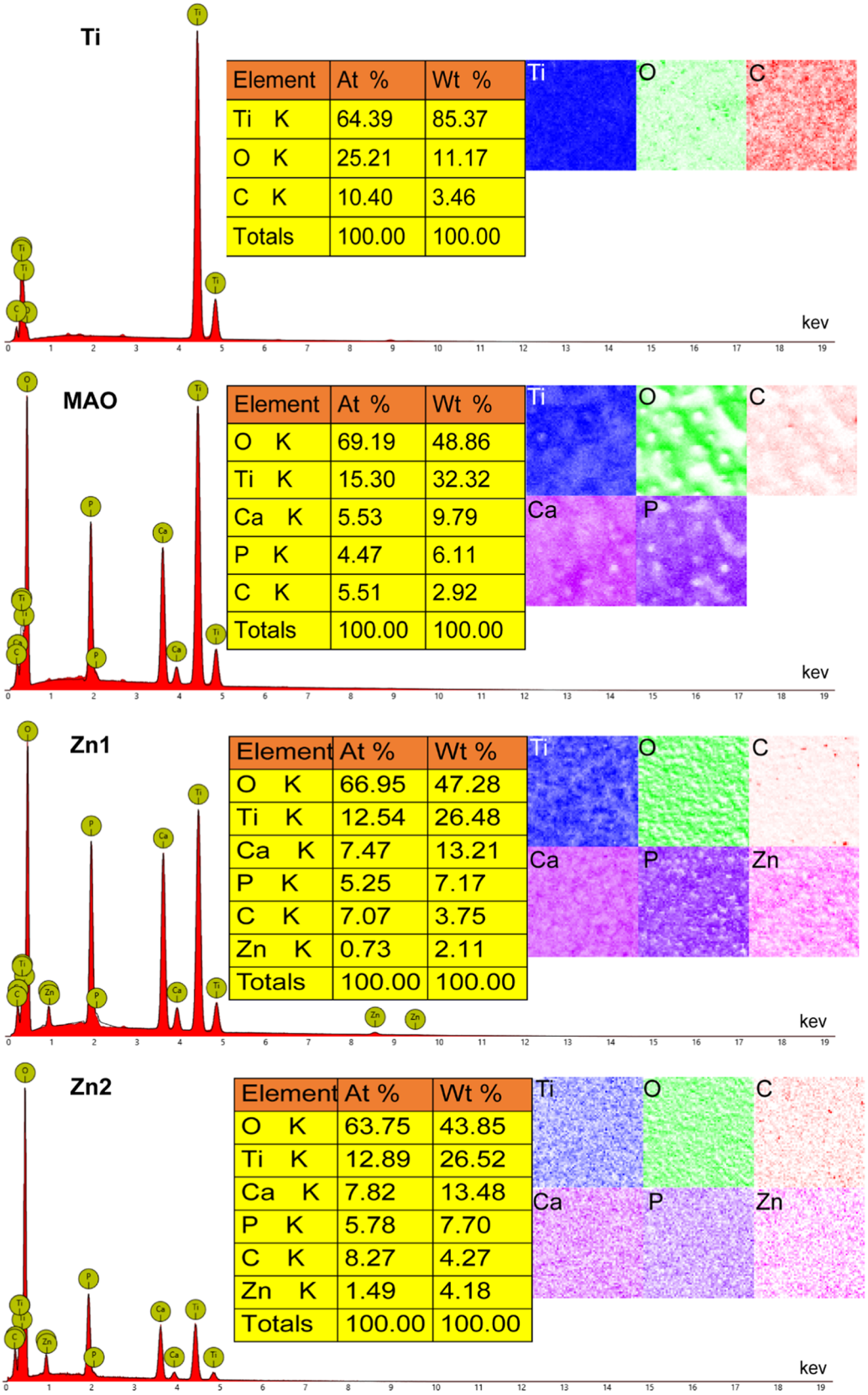

Figure 2. EDS elemental analysis of Ti, MAO, Zn1, and Zn2.

Premix EX Taq, Takara, Tokyo, Japan). GADPH was used to normalize the results. Data are expressed as fold change of the control according to equation $2^{-\Delta\Delta Ct}$. The primer sequences of the genes mentioned in the experiments are shown in Table 2.

2.13. Statistical Analysis. All of the above experiments were repeated at least three times, and the results were expressed as mean ± standard deviation (SD). They analyzed the results using Origin (Origin Lab Corporation, North-

https://doi.org/10.1021/acsomega.2c00579
ACS Omega 2022, 7, 14920−14932

ampton) software. One-way analysis of variance and multiple comparison tests were used to determine statistical significance. Statistically significant differences between groups and controls are indicated by "*". $^{\#}P$ suggests substantial differences between groups. "NS" indicates no significant difference.

3. RESULTS AND DISCUSSION

3.1. Surface Appearance. The chemical composition of the surface morphology and surface-modified structures is essential to achieve the bioactivity of the implants.[27,28] The surface morphology of each group was observed by SEM. The Ti group was the original morphology, and the MAO group, Zn1 group, and Zn2 group were treated with micro-arc oxidation to form a rough micro-arc oxidation coating on their surfaces (Figure 1a). The surface roughness of each group was observed by AFM, where the surface roughness was 39.7 nm for Ti, 512, 471.25, and 472.25 nm for the MAO group, Zn1, and Zn2, respectively. Compared to the Ti surface, the MAO group, Zn1, and Zn2 groups formed a rougher surface (Figure 1b). It has been demonstrated that the MAO treatment can slightly roughen the titanium surface at the microscale and significantly improve the surface hydrophilicity.[29−31]

The surface pore size (Figure 1c) and frequency distribution (Figure 1d) of each group were statistically analyzed by ImageJ. The pore sizes of the MAO group, Zn1, and Zn2 were 1.51 ± 0.72, 1.30 ± 0.65, and 1.57 ± 0.69 μm, respectively, and there was no statistical difference between the groups. The frequency distribution of pores in the Zn2 group was more uniform and consistent. It was shown that the microporous coating prepared from MAO significantly promoted cell adhesion and osteogenic differentiation.[32] In addition, the formed porous structure can provide the required spatial environment for the growth of different cells, thus promoting the proliferation and adhesion of most osteoblasts on the surface of the material.[11,33]

EDS observed the elemental composition of the surface of each group. No essential Zn was found in both the Ti and MAO groups, and in the Zn1 and Zn2 groups, Zn^{2+} was uniformly distributed on the coating surface and had been successfully incorporated into the microporous coating (Figure 2). In the elemental analysis, it was found that the fundamental composition ratio and the mass composition ratio of the Zn1 group were 0.73 and 2.11%, respectively; the elemental composition ratio and the mass composition ratio of the Zn^{2+} group were 1.49 and 4.18%, respectively. The percentage content of Zn^{2+} was nearly twice as high in the Zn2 group than in the Zn1 group, both in terms of elemental composition ratio and mass composition ratio. This is attributed to the fact that the content of zinc acetate in the electrolyte of the Zn2 group is twice the content of the Zn1 group, which further suggests that the coating indicates that the elemental content can be adjusted by adjusting the range of the components in the electrolyte. In addition, we also observed Ca and P in the MAO group, Zn1 group, and Zn2 group, which is because MAO can bind calcium (Ca) and phosphorus (P) to the generated oxide layer.[34]

3.1.1. Characterization of Surface Contact Angles for Different Groups. The surface contact angles were 73.55° ± 0.25, 25.74° ± 0.33, 15.52° ± 0.62, and 19.95° ± 0.48 for the Ti, MAO, Zn1, and Zn2 groups, respectively (Figure 3a,b). After micro-arc oxidation, the contact angle of the treated group was reduced and hydrophilicity was enhanced compared

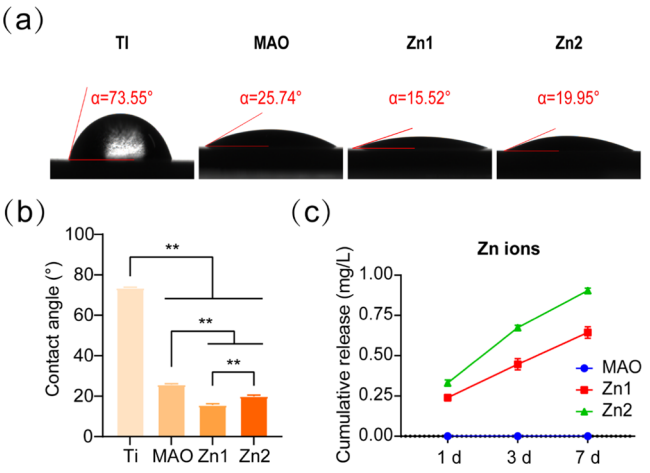

Figure 3. (a, b) Surface contact angles of Ti, MAO, Zn1, and Zn2. (c) ICP-OES examined the release of Zn^{2+} from the MAO, Zn1, and Zn2 groups on 1, 3, and 7 days. $^{**}P < 0.01$, $^{*}P$ indicates significant difference between groups.

to Ti. Among the treatment groups, the Zn1 group had the smallest contact angle of 15.52°, followed by the Zn2 group at 19.95°. It has been shown that the incorporation of tantalum (Ta) into micro-arc titanium oxide coatings improves the wettability of the coatings.[35] Therefore, this may be due to the addition of the Zn element, which reduces the surface contact angle and improves the wettability. For the Zn2 group, the contact angle was larger than that of the Zn1 group, with an average pore size of 1.57 μm for Zn2 and 1.30 μm for Zn1 (Figure 1d). It is considered that the pore size has an effect on the surface contact angle and it has also been pointed out in the literature that the pore morphology has an effect on the wettability aspect.[36,37]

3.2. Zn^{2+} Release. ICP-OES detected the release of Zn^{2+} at different time points. The concentrations of titanium in the Zn1 and Zn2 groups were 0.24 mg/L (3.7 μM), 0.45 mg/L (6.9 μM), 0.64 mg/L (9.8 μM), and 0.33 mg/L (5.1 μM), 0.67 mg/L (10 μM), and 0.90 mg/L (13.8 μM) for 1, 3, and 7 days of immersion in PBS, respectively. At every point in time, the Zn2 release was higher than Zn1. No Zn^{2+} was found in the Mao group (Figure 3c). The release curve shows that the release process of Zn is slow and continuous.

3.3. Cell Activity and Proliferation Experiment. *3.3.1. Analysis of Material Biocompatibility by CCK-8 Analysis and Live−Dead Cell Staining.* The OD values of BMSCs inoculated on the surface of the titanium sheets in each group on the first day were not significantly different between groups, confirming that the MAO-treated titanium sheets did not inhibit the growth of BMSCs in each group. The data on the third day showed that the cells in each group were in a continuous proliferation phase, with no significant differences between the MAO, Zn1, and Zn2 groups compared to Ti. However, the MAO group showed higher cell proliferation than the Zn2 group, which may be because the Zn elements were loaded on the surface of the coating and occupied a particular space, and the MAO group had more cover than the Zn2 group, promoting early cell proliferation. On day 7, the MAO and Zn2 groups showed a facilitative effect on BMSCs relative to the Ti group (Figure 4a).

The proliferation of BMSCs was examined by staining living and dead cells on the surface of different groups of titanium plates. After inoculating BMSCs in other groups for 1 day, a

https://doi.org/10.1021/acsomega.2c00579
ACS Omega 2022, 7, 14920−14932

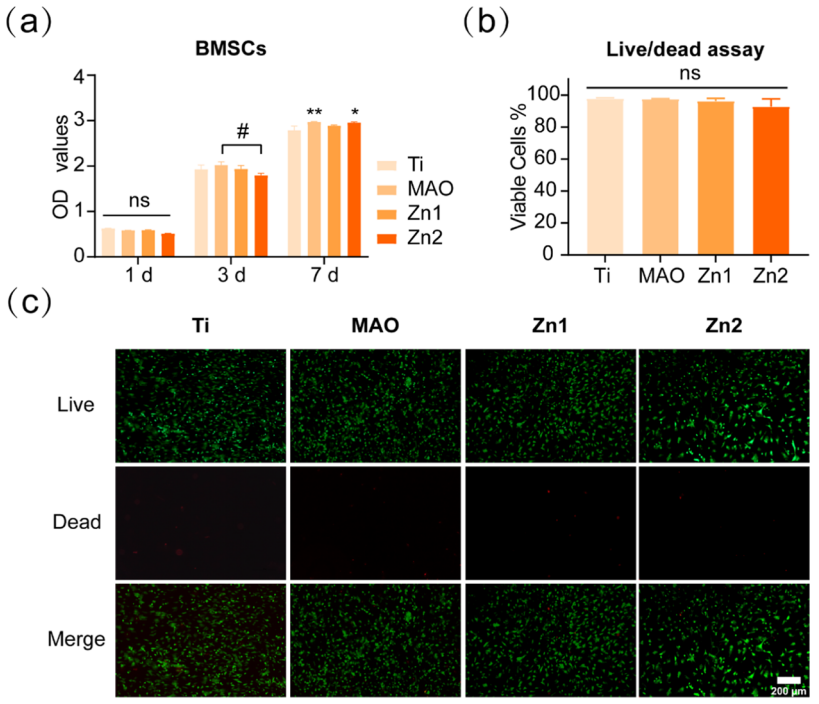

Figure 4. (a) BMSCs were cultured on different groups for CCK-8 analysis. (b, c) Live (green)−dead (red) cell staining and statistical analysis of BMSCs cultured on the titanium surface of different groups for 1 day. $^{*}P < 0.05$, $^{**}P < 0.01$, $^{*}P$ indicates a significant difference between the experimental and Ti groups; $^{\#}P$ indicates significant difference between groups; NS indicates no significant difference between the compared groups. Scale bar: 200 μm.

large number of living cells and a small number of dead cells were observed in each group (Figure 4c). Statistical analysis showed no significant difference in the proportion of living and dead cells (Figure 4b), indicating that the titanium plates treated by MAO had good biocompatibility.

The results of CCK-8 analysis and the staining of living and dead cells showed that the groups treated with MAO were relatively nontoxic to Ti and had good biocompatibility. Thus, for both the Zn1 and Zn2 groups, only Zn^{2+} was released from the biocompatibility. Previous studies have shown that BMSCs can survive well under 80 μm concentration of Zn^{2+}, higher than this value would be toxic to BMSCs.[17] Li et al. have shown that the response of BMSCs to zinc coating is highly dose-dependent.[38] The results showed that Zn^{2+} released from the Zn2-coated titanium micro-arc oxide coating was not toxic to BMSC proliferation and had good biological safety.

3.4. Cell Adhesion. By inoculating the cells on the surface of titanium, the growth of cells on the surface of titanium was observed. As shown in Figure 5a, we can see that the cells of the Ti group showed an overall long shuttle shape with a small cell spreading area after 12 h of growth on the surface of untreated titanium sheets. MAO, Zn1, and Zn2 treated with micro-arc oxidation had better cell extension and exhibited a better cell adhesion effect.

We also observed again the adhesion of BMSCs on Ti, MAO, Zn1, and Zn2 surfaces by TRITC selective binding to filamentous actin (F-actin; Figure 5b). Compared with the Ti group, MAO, Zn1, and Zn2 had better cell extension and showed better cell adhesion. Similar to cell growth on titanium sheets, it has been proved that the Mao treatment can change the wettability of the Ti surface, while the hydrophilic surface is easier for cell adhesion.[5,35] From the wettability point of view, the contact angle of the Zn2 group in the Zn1 group was smaller than those in the MAO group and Ti group, which was

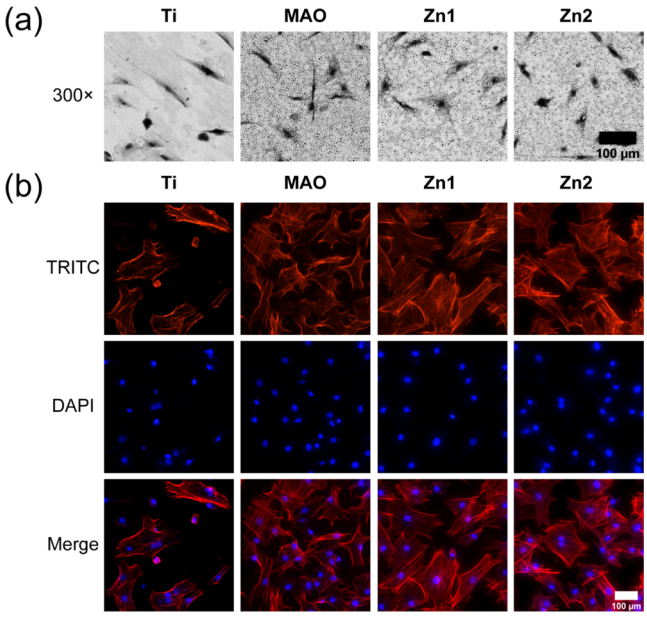

Figure 5. (a) BMSCs were photographed by SEM after 12 h of inoculation on the titanium surface of different groups. (b) Immunofluorescence staining of BMSCs after 24 h incubation on the titanium surface of different groups, TRITC (red) and DAPI (blue), is indicated by different colors. Scale bar: 100 μm.

consistent with the trend of the TRITC staining image. Therefore, it is likely that the Zn element is added, and the Zn1 group and Zn2 group have better adhesion than the MAO group.

Meanwhile, studies have shown that microporous coatings significantly enhance the initial bonding, proliferation, and osteogenic differentiation of BMSCs.[39] In most cases, a change

https://doi.org/10.1021/acsomega.2c00579
ACS Omega 2022, 7, 14920−14932

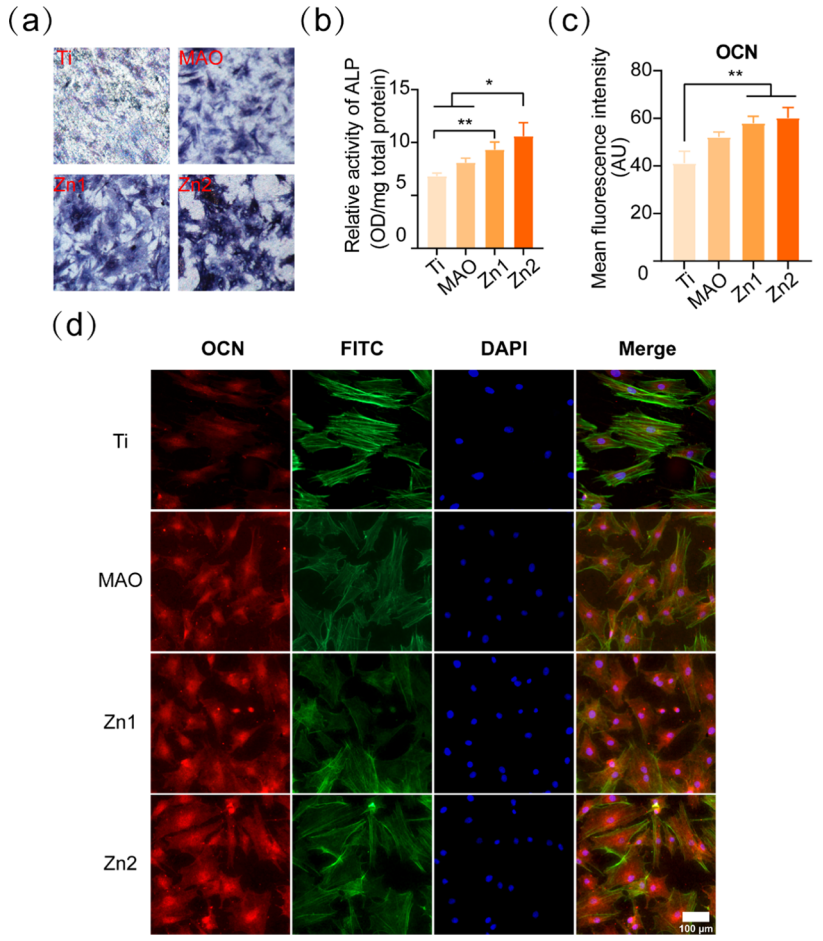

Figure 6. (a) ALP-stained images of BMSCs 7 days after inoculation on Ti, MAO, Zn1, and Zn2 surfaces (×50). (b) Quantitative analysis of ALP protein after 7 days of inoculation of BMSCs onto Ti, MAO, Zn1, and Zn2 surfaces. (c) Quantitative analysis of the average fluorescence intensity of OCN after 7 days of inoculation of BMSCs onto Ti, MAO, Zn1, and Zn2 surfaces. (d) OCN immunofluorescence staining, OCN (red), FITC (green), and DAPI (blue), indicated by different colors. *P < 0.05, **P < 0.01, *P indicates significant difference between groups. Scale bar: 100 μm.

in one aspect of the surface of a material is always accompanied by a significant difference in the properties of the other, making it difficult to determine the main factors that influence the response of the cell.[40] Therefore, the better physical properties of the MAO group, Zn1 group, and Zn2 group are also the result of various influences.

3.5. Osteogenesis. ALP staining was used to observe the effect of different treatment groups of titanium sheets on the early osteogenic effect of BMSCs. ALP was used as an indicator of early osteogenesis,[39] and the staining results showed that the Zn2 group had the darkest ALP staining, followed by the Zn1 and MAO groups, and finally by the pure titanium group (Figure 6a). The protein quantification results showed that the ALP protein expression was higher in the Zn1 and Zn2 groups than in the Ti group, but the Zn2 group also had a statistically significant increase relative to the MAO group (Figure 6b). This indicates that the Zn1 and Zn2 groups had good early osteogenesis, and the osteogenic effect was enhanced with increasing Zn concentration. It was found that Zn^{2+} at 10.91−27.15 μM in cell culture medium significantly improved the proliferation and ALP activity of mBMSCs, and high concentration (128.58 μM) of Zn^{2+} significantly inhibited ALP activity.[41] In ICP-OES ion release, the cumulative Zn^{2+} release concentrations of 9.8 and 13.8 μM for Zn1 and Zn2 on day 7 were within the appropriate range, consistent with the previous study.[41]

3.5.1. OCN Immunofluorescence Staining Analysis of the Effect of Different Treatment Groups of Titanium Sheets on the Late Osteogenesis of BMSCs. The expression of OCN protein in the Zn1 and Zn2 groups was significantly higher than that of OCN protein in the Ti group (Figure 6c,d). The above results confirmed that MAO we did prepare had a good osteogenesis-promoting effect in early and late osteogenesis of BMSCs, and the osteogenic effect was more significant due to the addition of Zn^{2+}.

3.6. Expression of Osteogenic Gene. On day 7, there was no significant difference in ALP, Osterix, and OCN expression between MAO and Ti groups. However, ALP, Osterix, and OCN expression were significantly higher in the Zn1 and Zn2 groups relative to the Ti group at this time point. On the 14th day, the promotive effect of the MAO group on Col-I, Osterix, and OCN was evident compared with the TI group, and ALP, Col-I, Osterix, and OCN were also higher in Zn1 and Zn2 groups than in TI and Mao groups. At the same time, the expression of ALP, Col-I, and OCN in the Zn2 group was better than that in the Zn1 group. The results show that the zinc-doped micro-arc oxidation coating prepared by us has a good osteogenesis effect, and the Zn2 group has the best osteogenesis effect (Figure 7).

https://doi.org/10.1021/acsomega.2c00579
ACS Omega 2022, 7, 14920−14932

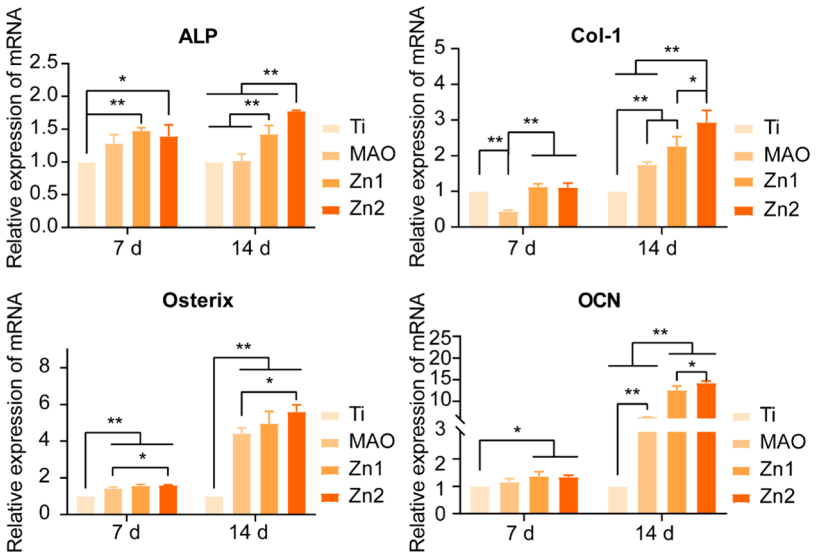

Figure 7. Expression of osteogenic genes associated with BMSCs after 7 and 14 days of Ti, MAO, Zn1, and Zn2 culture: ALP, COL-I, Osterix, and OCN. *P < 0.05, **P < 0.01, *P indicates significant difference between groups.

It has been proved that the HA coating formed by Mao has good osteogenesis.[28] We prepared zinc-coated micro-arc titanium oxide coating, which showed excellent bone-forming ability. ALP staining, ALP semiquantitative analysis, and ALP gene expression showed that the zinc-containing Mao group had a better impact on early bone regeneration. OCN is explicitly expressed in osteoblasts.[42−44] Both Zn1 and Zn2 showed a good osteogenic effect on Ti in OCN immunofluorescence staining, and the expression of the OCN gene was higher in the Zn2 group than that in the Zn1 group on 14 days. It is confirmed that Zn-loaded micro-arc titanium oxide coating can promote bone regeneration of BMSCs, and it is related to Zn element and concentration to some extent. In addition, both Col-I and Osterix are osteogenic genes,[45,46] and their gene expression trends also indicate this problem. This is further evidence that the Zn2 group has a better osteogenic effect. It has been shown that zinc induces osteogenesis, probably by Zn^{2+} activation of the cAMP-PKA pathway and the Gαq-PLC-AKT pathway, promoting cell survival/growth, differentiation, and osteogenic regeneration. This mainly triggers intracellular Ca^{2+} response, leading to MAPK activation.[47]

3.7. Anti-Inflammatory Effect. RAW264.7 cells were inoculated onto Ti, MAO, Zn1, and Zn2 surfaces to observe the growth of RAW264.7 on the covers of different treatment groups. Statistical analysis of CCK-8 at 1 day of inoculation revealed no significant effect on the development of RAW264.7 between the treatment groups relative to the Ti group (Figure 8a). This result was further validated by live−dead cell staining of RAW264.7 and statistical analysis (Figure 8b,c). The survival of RAW264.7 cells alone on the treated titanium surface of each group was not affected, and there was no significant promotion or inhibition.

Researchers widely use RAW264.7 macrophage-like cell lines to study macrophage polarization and immune regulation.[48] These mainly include the classical proinflammatory M1 and the alternative anti-inflammatory, wound healing M2.[49,50] Interferon-γ (IFN-γ) or lipopolysaccharide (LPS) induces proinflammatory M1 macrophages, usually with the surface marker CD86, and they promote inflammation by

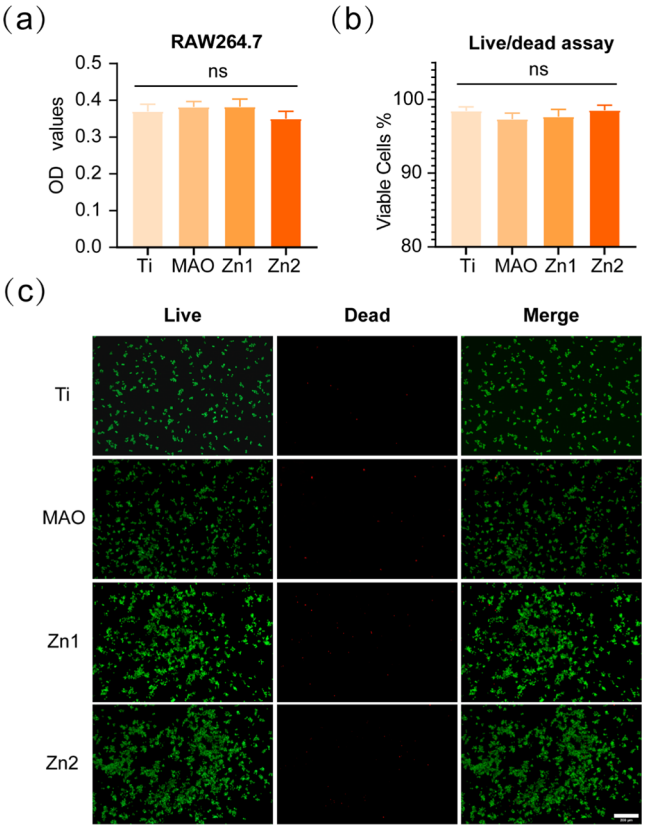

Figure 8. (a) RAW264.7 was cultured on different groups for CCK-8 analysis. (b, c) Live−dead cell staining and statistical analysis of RAW264.7 cultured on the titanium surface of different groups for 1 day. NS indicates no significant difference between the compared groups. Scale bar: 200 μm.

releasing inflammatory cytokines (IL-1β, IL-6, iNOS, and TNF-α), reactive oxygen species, and antimicrobial peptides.[51−53] Anti-inflammatory M2 macrophages are induced by IL-4 and can inhibit inflammation by releasing anti-inflammatory mediators arginase-1 (Arg-1) and interleukin

https://doi.org/10.1021/acsomega.2c00579
ACS Omega 2022, 7, 14920−14932

10 (IL-10) via the surface marker mannose receptor (CD206).[54,55]

The expression of inflammatory genes was detected by q-PCR. After RAW264.7 inoculation on Ti, MAO, Zn1, and Zn2 surfaces for 24 h, there was a downregulation trend of CD86, INOS, and TNF-α (Figure 9). Among them, the Zn2 group showed the most downregulation compared to the Ti group, followed by the Zn1 group, and the MAO group also showed a slight downregulation, suggesting that the MAO, Zn1, and Zn2 groups showed anti-inflammatory effects. CD86, a gene that acts as a proinflammatory factor, was downregulated by inoculating RAW264.7 cells on the surface of MAO, which may be associated with increased roughness of the MAO surface. Related studies have shown that increased surface roughness indirectly promotes the polarization of M2-activated macrophages.[5]

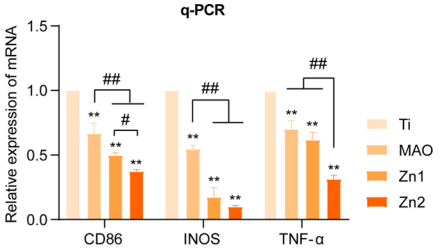

Figure 9. Expression of relevant proinflammatory genes; CD86, INOS, and TNF-α after inoculation of RAW264.7 with incubation on Ti, MAO, Zn1, and Zn2 surfaces for 24 h. *P indicates statistical difference in the treatment group compared to the Ti group and is consistent with **$P < 0.01$. $^{\#}P$ indicates significant difference between groups and is consistent with $P < 0.05$ and $^{\#\#}P < 0.01$.

In contrast, both the Zn1 and Zn2 groups showed downregulation of CD86 relative to MAO, indicating that the addition of Zn ions did act as an anti-inflammatory agent. The anti-inflammatory effect was more pronounced in the high Zn2 concentration group in the present study. The same trend was shown for the proinflammatory genes INOS and TNF-α.

It has been shown that excessively elevated inflammatory markers, reactive oxygen species, and antimicrobial peptides are associated with increased serum hypozincemia.[56] Zinc is the second messenger comparable to calcium, and changes in intracellular zinc concentration alter cell signaling. Intracellular levels of free zinc affect the signaling pathway by reversibly binding to regulatory sites of signaling proteins and altering protein activity and stability.[57,58] Related studies have shown that nuclear factor kappa B (NF-κB), a transcription factor, is a significant regulator of the proinflammatory response and that zinc is involved in regulating the proinflammatory response by targeting NF-κB.[59]

3.8. Zn^{2+} Anti-Inflammatory Concentration Screening. By inoculating RAW264.7 cells on the surface of the micro-arc titanium oxide coating, the study showed that micro-arc titanium oxide containing zinc had a better anti-inflammatory effect. At the same time, the high concentration of the Zn2 group had a better anti-inflammatory effect than the low concentration of the Zn1 group. This stimulated our interest in the anti-inflammatory effect of Zn^{2+}. Moreover, the effect of different concentrations of Zn^{2+} on the expression of RAW264.7-related inflammatory factors has not been clarified, which also prompted our interest in exploring the effect of different concentrations of Zn^{2+} on the expression of RAW264.7-related inflammatory factors. To this end, we performed in vitro validation of the anti-inflammatory effect of Zn^{2+} to screen the optimal anti-inflammatory concentration of Zn^{2+}. First, the biosafe concentrations of Zn^{2+} for RAW264.7 were screened by CCK-8 analysis. CCK-8 analysis on day 1 showed (Figure 10a) that Zn^{2+} significantly inhibited the proliferation of RAW264.7 at Zn^{2+} concentrations of 140, 160, and 180 μM. CCK-8 analysis on day 3 showed (Figure 10a) that Zn^{2+} also showed a significant inhibitory effect on RAW264.7 proliferation at concentrations of 120 μM and above. The results showed that five concentration groups of 100 μm and below 40, 60, and 80 μm were selected for anti-inflammatory study in vitro.

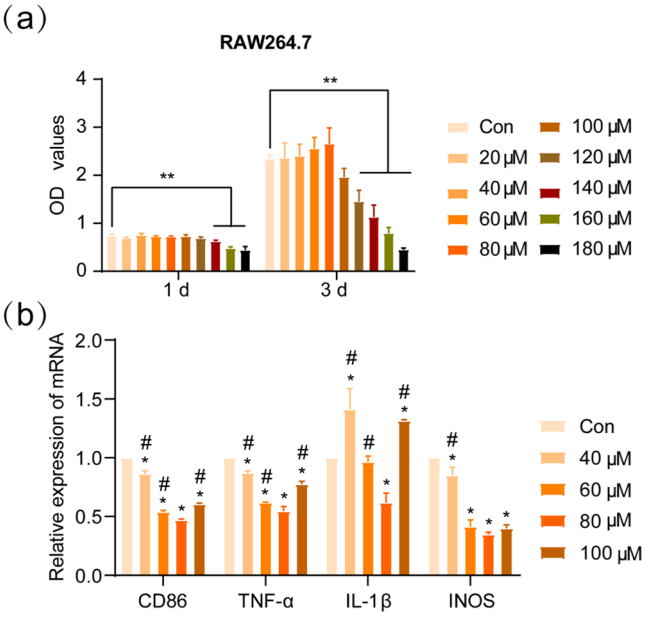

Figure 10. (a) RAW264.7 was incubated in DMEM containing Zn^{2+} at different concentrations for CCK-8 analysis. (b) RAW264.7 was cultured in screened Zn^{2+}-containing DMEM to see the expression of relevant inflammatory genes: CD86, INOS, TNF-α, and INOS. *P indicates a statistical difference between the different Zn^{2+} groups compared to the blank control (Con) group, consistent with $*P < 0.05$. $^{\#}P$ suggests a statistical difference in the other Zn^{2+} groups compared to the 80 μM group, compatible with $^{\#}P < 0.05$.

We verified the effects of different concentrations of Zn^{2+} groups on the expression of RAW264.7 cell-associated proinflammatory factors under in vitro conditions by q-PCR. The results showed (Figure 10b) that the expression of CD86, TNF-α, and INOS was downregulated in each concentration group relative to the blank control group, all of which were statistically significant. In IL-1β expression, only the 80 μM concentration group was downregulated compared to the blank control. The 80 μM concentration group showed the greatest downregulation of CD86, TNF-α, IL-1β, and INOS expression compared with the other groups. In the present study, we investigated the effect of Zn^{2+} on the expression of RAW264.7-related proinflammatory factors in vitro and found that the 80 μM concentration group had the best effect on the downregulation of proinflammatory factors. In addition, at Zn^{2+} concentration below 80 μM, the closer the concentration to 80 μM, the stronger the effect of inhibiting the expression of proinflammatory factors, while above 80 μM, the effect of

https://doi.org/10.1021/acsomega.2c00579
ACS Omega 2022, 7, 14920−14932

inhibiting the expression of proinflammatory factors was reduced.

In the present study, elemental Zn was loaded on the surface of titanium flakes by micro-arc oxidation. By detecting the ion release concentration (Figure 3c), we found that the cumulative release concentration was 0.64 mg/L (9.8 μM) and 0.90 mg/L (13.8 μM) for 7 days in the Zn1 and Zn2 groups, respectively, and the Zn2 group was higher than the Zn1 group within 80 μM. The Zn2 group showed better inhibition of inflammation than the Zn1 group by q-PCR to detect the expression of relevant proinflammatory-related factors CD86, TNF-α, and INOS (Figure 9). Consistent with the trend of inhibition of proinflammatory factor expression by Zn^{2+} in vitro, it also indirectly verified that the inhibitory effect of zinc-coated micro-arc titanium oxide on inflammation under certain conditions was correlated with the concentration of Zn^{2+} release.

4. CONCLUSIONS

In this study, zinc-coated titanium micro-arc oxide coatings were prepared by MAO, which has good biocompatibility and inhibits the expression of inflammatory genes. To evaluate the anti-inflammatory effect of zinc-coated micro-arc titanium oxide, we cultured RAW264.7 cells on the surface of zinc-coated micro-arc titanium oxide and examined the expression of related inflammatory genes. The results showed that the Zn2 group ($Zn(CH_3COO)_2{\cdot}2H_2O$ concentration of 10 mmol/L) had a better inhibitory effect on the expression of inflammatory genes. Meanwhile, it was found that zinc-coated micro-arc titanium oxide in the Zn2 group had better bone-enabling results relative to the Zn1 group through in vitro studies. In addition, we further screened the optimal concentration of Zn^{2+} anti-inflammatory in vitro and confirmed that 80 μM of Zn^{2+} has the optimal inhibitory effect on inflammatory gene expression, preparing for the clinical application of Zn^{2+} anti-inflammatory. In a word, the coating designed by us has good anti-inflammation and bone-forming effect, which is successful application research of surface modification of titanium.

AUTHOR INFORMATION

Corresponding Authors

Jingzhou Hu − *Department of Oral & Maxillofacial-Head & Neck Oncology, Ninth People's Hospital, Shanghai Jiao Tong University School of Medicine, Shanghai 200011, China;* orcid.org/0000-0003-4402-3370; Email: huyayi@shsmu.edu.cn

Lei Shi − *Department of Oral and Maxillofacial Surgery, Gansu Provincial Hospital, Lanzhou 730000, China;* Email: shileigansu@163.com

Honghai Ji − *School of Stomatology, Weifang Medical University, Weifang 261053 Shandong, China;* Email: sdwf_ji@wfmc.edu.cn

Authors

Haishui Sun − *School of Stomatology, Weifang Medical University, Weifang 261053 Shandong, China;* orcid.org/0000-0002-4516-6309

Yiming Yang − *College of Stomatology, Shanghai Jiao Tong University, National Center for Stomatology, Shanghai 200011, China; National Clinical Research Center for Oral Diseases, Shanghai 200011, China; Shanghai Key Laboratory of Stomatology, Shanghai 200072, China; Department of Orthodontics, Shanghai Ninth People's Hospital, Shanghai Jiao Tong University School of Medicine, Shanghai 200025, China*

Lei Yu − *School of Stomatology, Weifang Medical University, Weifang 261053 Shandong, China*

Ke Liu − *School of Stomatology, Weifang Medical University, Weifang 261053 Shandong, China*

Yifan Fei − *Department of Oral & Maxillofacial-Head & Neck Oncology, Ninth People's Hospital, Shanghai Jiao Tong University School of Medicine, Shanghai 200011, China*

Chaoyang Guo − *School of Stomatology, Weifang Medical University, Weifang 261053 Shandong, China*

Yuqi Zhou − *School of Stomatology, Weifang Medical University, Weifang 261053 Shandong, China*

Complete contact information is available at: https://pubs.acs.org/10.1021/acsomega.2c00579

Author Contributions

○H.S. and Y.Y. contributed equally to this work and should be considered co-first authors.

Notes

The authors declare no competing financial interest.

ACKNOWLEDGMENTS

This study was supported by the "Crossover" Research Fund of the Ninth People's Hospital of Shanghai Jiao Tong University (No. JYJC202102) and the Natural Science Foundation of Gansu Province (No. 21JR1RA030).

REFERENCES

(1) Liu, X. H.; Wu, L.; Ai, H. J.; Han, Y.; Hu, Y. Cytocompatibility and early osseointegration of nanoTiO2-modified Ti-24 Nb-4 Zr-7.9 Sn surfaces. *Mater. Sci. Eng., C* **2015**, *48*, 256−262.

(2) Zhang, W.; Cao, H.; Zhang, X.; Li, G.; Chang, Q.; Zhao, J.; Qiao, Y.; Ding, X.; Yang, G.; Liu, X.; Jiang, X. A strontium-incorporated nanoporous titanium implant surface for rapid osseointegration. *Nanoscale* **2016**, *8*, 5291−5301.

(3) Zhao, Q.; Yi, L.; Jiang, L.; Ma, Y.; Lin, H.; Dong, J. Surface functionalization of titanium with zinc/strontium-doped titanium dioxide microporous coating via microarc oxidation. *Nanomedicine* **2019**, *16*, 149−161.

(4) Albrektsson, T.; Dahlin, C.; Jemt, T.; Sennerby, L.; Turri, A.; Wennerberg, A. Is marginal bone loss around oral implants the result of a provoked foreign body reaction? *Clin. Implant Dent. Relat. Res.* **2014**, *16*, 155−165.

(5) Hotchkiss, K. M.; Reddy, G. B.; Hyzy, S. L.; Schwartz, Z.; Boyan, B. D.; Olivares-Navarrete, R. Titanium surface characteristics, including topography and wettability, alter macrophage activation. *Acta Biomater.* **2016**, *31*, 425−434.

(6) Mavrogenis, A. F.; Dimitriou, R.; Parvizi, J.; Babis, G. C. Biology of implant osseointegration. *J. Musculoskeletal Neuronal Interact.* **2009**, *9*, 61−71.

(7) Chen, Z.; Klein, T.; Murray, R. Z.; Crawford, R.; Chang, J.; Wu, C.; Xiao, Y. Osteoimmunomodulation for the development of advanced bone biomaterials. *Mater. Today* **2016**, *19*, 304−321.

(8) Eger, M.; Hiram-Bab, S.; Liron, T.; Sterer, N.; Carmi, Y.; Kohavi, D.; Gabet, Y. Mechanism and Prevention of Titanium Particle-Induced Inflammation and Osteolysis. *Front. Immunol.* **2018**, *9*, No. 2963.

(9) Yin, Y.; He, X.-T.; Wang, J.; Wu, R.-X.; Xu, X.-Y.; Hong, Y.-L.; Tian, B.-M.; Chen, F.-M. Pore size-mediated macrophage M1-to-M2 transition influences new vessel formation within the compartment of a scaffold. *Appl. Mater. Today* **2020**, *18*, No. 100466.

(10) Kang, H.; Kim, S.; Wong, D. S. H.; Jung, H. J.; Lin, S.; Zou, K.; Li, R.; Li, G.; Dravid, V. P.; Bian, L. Remote Manipulation of Ligand

Nano-Oscillations Regulates Adhesion and Polarization of Macrophages in Vivo. *Nano Lett.* **2017**, *17*, 6415−6427.
(11) Gittens, R. A.; McLachlan, T.; Olivares-Navarrete, R.; Cai, Y.; Berner, S.; Tannenbaum, R.; Schwartz, Z.; Sandhage, K. H.; Boyan, B. D. The effects of combined micron-/submicron-scale surface roughness and nanoscale features on cell proliferation and differentiation. *Biomaterials* **2011**, *32*, 3395−3403.
(12) Premanathan, M.; Karthikeyan, K.; Jeyasubramanian, K.; Manivannan, G. Selective toxicity of ZnO nanoparticles toward Gram-positive bacteria and cancer cells by apoptosis through lipid peroxidation. *Nanomedicine* **2011**, *7*, 184−192.
(13) Jin, G.; Cao, H.; Qiao, Y.; Meng, F.; Zhu, H.; Liu, X. J. C.; Biointerfaces, S. B. Osteogenic activity and antibacterial effect of zinc ion implanted titanium. *Colloids Surf., B* **2014**, *117*, 158−165.
(14) Hyun-Ju, S.; Young-Eun, C.; Taewan, K.; Hong-In, S.; In-Sook, K. J. N. R. Practice, Zinc may increase bone formation through stimulating cell proliferation, alkaline phosphatase activity and collagen synthesis in osteoblastic MC3T3-E1. *Nutr. Res. Pract.* **2010**, *4*, 356−361.
(15) Fielding, G. A.; Smoot, W.; Bose, S. Effects of SiO2, SrO, MgO, and ZnO dopants in tricalcium phosphates on osteoblastic Runx2 expression. *J. Biomed. Mater. Res., Part A* **2014**, *102*, 2417−2426.
(16) Grandjean-Laquerriere, A.; Laquerriere, P.; Jallot, E.; Nedelec, J. M.; Guenounou, M.; Laurent-Maquin, D.; Phillips, T. M. Influence of the zinc concentration of sol-gel derived zinc substituted hydroxyapatite on cytokine production by human monocytes in vitro. *Biomaterials* **2006**, *27*, 3195−3200.
(17) Yin, S.; Sun, N.; Jiang, F.; Lu, Y.; Yang, G.; Wu, X.; Lin, S.; Zhang, W.; Jiang, X. The Translation from In Vitro Bioactive Ion Concentration Screening to In Vivo Application for Preventing Peri-implantitis. *ACS Appl. Mater. Interfaces* **2021**, *13*, 5782−5794.
(18) Liu, W.; Li, J.; Cheng, M.; Wang, Q.; Yeung, K. W. K.; Chu, P. K.; Zhang, X. Zinc-Modified Sulfonated Polyetheretherketone Surface with Immunomodulatory Function for Guiding Cell Fate and Bone Regeneration. *Adv. Sci.* **2018**, *5*, No. 1800749.
(19) Zhang, Y. Y.; Zhu, Y.; Lu, D. Z.; Dong, W.; Bi, W. J.; Feng, X. J.; Wen, L. M.; Sun, H.; Qi, M. C. Evaluation of osteogenic and antibacterial properties of strontium/silver-containing porous TiO2 coatings prepared by micro-arc oxidation. *J. Biomed. Mater. Res., Part B* **2021**, *109*, 505−516.
(20) Bai, L.; Du, Z.; Du, J.; Yao, W.; Zhang, J.; Weng, Z.; Liu, S.; Zhao, Y.; Liu, Y.; Zhang, X. J. B. A multifaceted coating on titanium dictates osteoimmunomodulation and osteo/angio-genesis towards ameliorative osseointegration. *Biomaterials* **2018**, *162*, 154−169.
(21) Khrunyk, Y. Y.; Belikov, S. V.; Tsurkan, M. V.; Vyalykh, I. V.; Markaryan, A. Y.; Karabanalov, M. S.; Popov, A. A.; Wysokowski, M. Surface-Dependent Osteoblasts Response to TiO2 Nanotubes of Different Crystallinity. *Nanomaterials* **2020**, *10*, No. 320.
(22) Shen, X.; Hu, W.; Ping, L.; Liu, C.; Yao, L.; Deng, Z.; Wu, G. Antibacterial and Osteogenic Functionalization of Titanium With Silicon/Copper-Doped High-Energy Shot Peening-Assisted Micro-Arc Oxidation Technique. *Front. Bioeng. Biotechnol.* **2020**, *8*, No. 573464.
(23) Xue, T.; Attarilar, S.; Liu, S.; Liu, J.; Song, X.; Li, L.; Zhao, B.; Tang, Y. Surface Modification Techniques of Titanium and its Alloys to Functionally Optimize Their Biomedical Properties: Thematic Review. *Front. Bioeng. Biotechnol.* **2020**, *8*, No. 603072.
(24) Wang, R.; He, X.; Gao, Y.; Zhang, X.; Yao, X.; Tang, B. Antimicrobial property, cytocompatibility and corrosion resistance of Zn-doped ZrO2/TiO2 coatings on Ti6Al4V implants. *Mater. Sci. Eng., C* **2017**, *75*, 7−15.
(25) Zhang, R.; Xu, N.; Liu, X.; Yang, X.; Yan, H.; Ma, J.; Feng, Q.; Shen, Z. Micro/nanostructured TiO2/ZnO coating enhances osteogenic activity of SaOS-2 cells. *Artif. Cells, Nanomed., Biotechnol.* **2019**, *47*, 2838−2845.
(26) Zhang, R.; Liu, X.; Xiong, Z.; Huang, Q.; Yang, X.; Yan, H.; Ma, J.; Feng, Q.; Shen, Z. Novel micro/nanostructured TiO2/ZnO coating with antibacterial capacity and cytocompatibility. *Ceram. Int.* **2018**, *44*, 9711−9719.
(27) Xu, J. Y.; Chen, X. S.; Zhang, C. Y.; Liu, Y.; Wang, J.; Deng, F. L. Improved bioactivity of selective laser melting titanium: Surface modification with micro-/nano-textured hierarchical topography and bone regeneration performance evaluation. *Mater. Sci. Eng., C* **2016**, *68*, 229−240.
(28) Lu, M.; Chen, H.; Yuan, B.; Zhou, Y.; Min, L.; Xiao, Z.; Zhu, X.; Tu, C.; Zhang, X. Electrochemical Deposition of Nanostructured Hydroxyapatite Coating on Titanium with Enhanced Early Stage Osteogenic Activity and Osseointegration. *Int. J. Nanomed.* **2020**, *15*, 6605−6618.
(29) He, W.; Yin, X.; Xie, L.; Liu, Z.; Li, J.; Zou, S.; Chen, J. J. J. oM. S. M. iM. Enhancing osseointegration of titanium implants through large-grit sandblasting combined with micro-arc oxidation surface modification. *J. Mater. Sci.: Mater. Med.* **2019**, *30*, No. 73.
(30) Schneider, G. B.; Perinpanayagam, H.; Clegg, M.; Zaharias, R.; Seabold, D.; Keller, J.; Stanford, C. Implant surface roughness affects osteoblast gene expression. *J. Dent. Res.* **2003**, *82*, 372−376.
(31) Wennerberg, A.; Hallgren, C.; Johansson, C.; Danelli, S. A histomorphometric evaluation of screw-shaped implants each prepared with two surface roughnesses. *Clin. Oral Implants Res.* **1998**, *9*, 11−19.
(32) Zhou, W.; Huang, O.; Gan, Y.; Li, Q.; Zhou, T.; Xi, W. Effect of titanium implants with coatings of different pore sizes on adhesion and osteogenic differentiation of BMSCs. *Artif. Cells, Nanomed., Biotechnol.* **2019**, *47*, 290−299.
(33) Li, X.; Wang, M.; Zhang, W.; Bai, Y.; Liu, Y.; Meng, J.; Zhang, L. A Magnesium-Incorporated Nanoporous Titanium Coating for Rapid Osseointegration. *Int. J. Nanomed.* **2020**, *15*, 6593−6603.
(34) Shimabukuro, M.; Tsutsumi, H.; Tsutsumi, Y.; Manaka, T.; Chen, P.; Ashida, M.; Ishikawa, K.; Katayama, H.; Hanawa, T. Enhancement of antibacterial property of titanium by two-step micro arc oxidation treatment. *Dent. Mater. J.* **2021**, *40*, 592−598.
(35) Lu, R. J.; Wang, X.; He, H. X.; E, L. L.; Li, Y.; Zhang, G. L.; Li, C. J.; Ning, C. Y.; Liu, H. C. Tantalum-incorporated hydroxyapatite coating on titanium implants: its mechanical and in vitro osteogenic properties. *J. Mater. Sci.: Mater. Med.* **2019**, *30*, No. 111.
(36) Cho, W. K.; Choi, I. S. Fabrication of Hairy Polymeric Films Inspired by Geckos: Wetting and High Adhesion Properties. *Adv. Funct. Mater.* **2008**, *18*, 1089−1096.
(37) Saji, V. S. Superhydrophobic surfaces and coatings by electrochemical anodic oxidation and plasma electrolytic oxidation. *Adv. Colloid Interface Sci.* **2020**, *283*, No. 102245.
(38) Li, S.; Chen, X.; Wang, X.; Xiong, Y.; Yan, Y.; Tan, Z.; Yang, X.; Li, Y. Simonkolleite Coating on Poly(Amino Acids) to Improve Osteogenesis and Suppress Osteoclast Formation in Vitro. *Polymers* **2019**, *11*, No. 1505.
(39) Zhou, W.; Wang, T.; Gan, Y.; Yang, J.; Zhu, H.; Wang, A.; Wang, Y.; Xi, W. Effect of micropore/microsphere topography and a silicon-incorporating modified titanium plate surface on the adhesion and osteogenic differentiation of BMSCs. *Artif. Cells, Nanomed., Biotechnol.* **2020**, *48*, 230−241.
(40) Zhang, W.; Wang, G.; Liu, Y.; Zhao, X.; Zou, D.; Zhu, C.; Jin, Y.; Huang, Q.; Sun, J.; Liu, X.; Jiang, X.; Zreiqat, H. The synergistic effect of hierarchical micro/nano-topography and bioactive ions for enhanced osseointegration. *Biomaterials* **2013**, *34*, 3184−3195.
(41) Xiong, K.; Zhang, J.; Zhu, Y.; Chen, L.; Ye, J. Zinc doping induced differences in the surface composition, surface morphology and osteogenesis performance of the calcium phosphate cement hydration products. *Mater. Sci. Eng., C* **2019**, *105*, No. 110065.
(42) Lin, S.; Yang, G.; Jiang, F.; Zhou, M.; Yin, S.; Tang, Y.; Tang, T.; Zhang, Z.; Zhang, W.; Jiang, X. A Magnesium-Enriched 3D Culture System that Mimics the Bone Development Microenvironment for Vascularized Bone Regeneration. *Adv. Sci.* **2019**, *6*, No. 1900209.
(43) Komori, T. Functions of Osteocalcin in Bone, Pancreas, Testis, and Muscle. *Int. J. Mol. Sci.* **2020**, *21*, No. 7513.
(44) Han, Y.; You, X.; Xing, W.; Zhang, Z.; Zou, W. Paracrine and endocrine actions of bone-the functions of secretory proteins from osteoblasts, osteocytes, and osteoclasts. *Bone Res.* **2018**, *6*, No. 16.

https://doi.org/10.1021/acsomega.2c00579
ACS Omega 2022, 7, 14920−14932

(45) Song, Y.; Wu, H.; Gao, Y.; Li, J.; Lin, K.; Liu, B.; Lei, X.; Cheng, P.; Zhang, S.; Wang, Y.; Sun, J.; Bi, L.; Pei, G. Zinc Silicate/Nano-Hydroxyapatite/Collagen Scaffolds Promote Angiogenesis and Bone Regeneration via the p38 MAPK Pathway in Activated Monocytes. *ACS Appl. Mater. Interfaces* **2020**, *12*, 16058−16075.
(46) Yang, G.; Yang, H.; Shi, L.; Wang, T.; Zhou, W.; Zhou, T.; Han, W.; Zhang, Z.; Lu, W.; Hu, J. Enhancing Corrosion Resistance, Osteoinduction, and Antibacterial Properties by Zn/Sr Additional Surface Modification of Magnesium Alloy. *ACS Biomater. Sci. Eng.* **2018**, *4*, 4289−4298.
(47) Zhu, D.; Su, Y.; Young, M. L.; Ma, J.; Zheng, Y.; Tang, L. Biological Responses and Mechanisms of Human Bone Marrow Mesenchymal Stem Cells to Zn and Mg Biomaterials. *ACS Appl. Mater. Interfaces* **2017**, *9*, 27453−27461.
(48) Hamlet, S.; Alfarsi, M.; George, R.; Ivanovski, S. The effect of hydrophilic titanium surface modification on macrophage inflammatory cytokine gene expression. *Clin. Oral Implants Res.* **2012**, *23*, 584−590.
(49) Martinez, F. O.; Gordon, S. The M1 and M2 paradigm of macrophage activation: time for reassessment. *F1000Prime Rep.* **2014**, *6*, No. 13.
(50) Murray, P. J.; Allen, J. E.; Biswas, S. K.; Fisher, E. A.; Gilroy, D. W.; Goerdt, S.; Gordon, S.; Hamilton, J. A.; Ivashkiv, L. B.; Lawrence, T.; Locati, M.; Mantovani, A.; Martinez, F. O.; Mege, J. L.; Mosser, D. M.; Natoli, G.; Saeij, J. P.; Schultze, J. L.; Shirey, K. A.; Sica, A.; Suttles, J.; Udalova, I.; van Ginderachter, J. A.; Vogel, S. N.; Wynn, T. A. Macrophage activation and polarization: nomenclature and experimental guidelines. *Immunity* **2014**, *41*, 14−20.
(51) Shapouri-Moghaddam, A.; Mohammadian, S.; Vazini, H.; Taghadosi, M.; Esmaeili, S. A.; Mardani, F.; Seifi, B.; Mohammadi, A.; Afshari, J. T.; Sahebkar, A. Macrophage plasticity, polarization, and function in health and disease. *J. Cell. Physiol.* **2018**, *233*, 6425−6440.
(52) Yuan, Y.; Jiang, Y.; Wang, B.; Guo, Y.; Gong, P.; Xiang, L. Deficiency of Calcitonin Gene-Related Peptide Affects Macrophage Polarization in Osseointegration. *Front. Physiol.* **2020**, *11*, No. 733.
(53) Hesketh, M.; Sahin, K. B.; West, Z. E.; Murray, R. Z. Macrophage Phenotypes Regulate Scar Formation and Chronic Wound Healing. *Int. J. Mol. Sci.* **2017**, *18*, No. 1545.
(54) Horwood, N. J. Macrophage Polarization and Bone Formation: A review. *Clin. Rev. Allergy Immunol.* **2016**, *51*, 79−86.
(55) Martin, K. E.; García, A. J. Macrophage phenotypes in tissue repair and the foreign body response: Implications for biomaterial-based regenerative medicine strategies. *Acta Biomater.* **2021**, *133*, 4−16.
(56) Wessels, I.; Cousins, R. J. Zinc dyshomeostasis during polymicrobial sepsis in mice involves zinc transporter Zip14 and can be overcome by zinc supplementation. *Am. J. Physiol.: Gastrointest. Liver Physiol.* **2015**, *309*, G768−G778.
(57) Maret, W. Metals on the move: zinc ions in cellular regulation and in the coordination dynamics of zinc proteins. *BioMetals* **2011**, *24*, 411−418.
(58) Yamasaki, S.; Sakata-Sogawa, K.; Hasegawa, A.; Suzuki, T.; Kabu, K.; Sato, E.; Kurosaki, T.; Yamashita, S.; Tokunaga, M.; Nishida, K.; Hirano, T. Zinc is a novel intracellular second messenger. *J. Cell Biol.* **2007**, *177*, 637−645.
(59) Gammoh, N. Z.; Rink, L. Zinc in Infection and Inflammation. *Nutrients* **2017**, *9*, No. 624.

https://doi.org/10.1021/acsomega.2c00579
ACS Omega 2022, 7, 14920−14932